UNSUPERVISED SEGMENTATION AND PERSONALISED FE MODELLING OF *IN VIVO* HUMAN MYOCARDIAL MECHANICS BASED ON AN MRI ATLAS

V.Y. Wang[1], C. Hoogendoorn[2], G. Engelbrecht[2], A.F. Frangi[2,4], A.A. Young[1], P.J. Hunter[1], M.P. Nash,[1,3]

[1]Auckland Bioengineering Institute, University of Auckland, New Zealand
[2] Center for Computational Imaging & Simulation Technologies in Biomedicine; Department of Information and Communication Technologies, Universitat Pompeu Fabra, Barcelona, Spain
[3] Department of Engineering Science, University of Auckland, New Zealand
[4] Department of Mechanical Engineering, University of Sheffield, Sheffield, UK

ABSTRACT

We have developed techniques to automatically generate personalised biomechanical models of patients' hearts based on 3D cardiac images. We demonstrate this approach using multi-slice computed tomography images. Unsupervised segmentation was performed using non-rigid image registration with a segmented image. A finite element model was automatically fitted to the segmented data of the left ventricle. Passive and contractile myocardial mechanical properties were tuned to match the segmented surface geometries at end-diastole and end-systole, respectively. Global and regional indices of myocardial mechanics, including cardiac wall and myofibre strain distributions, were then quantified. This automated biomechanical modelling approach to cardiac image analysis provided noninvasive methods to characterise heart function, and may provide new quantitative diagnostic markers for heart failure.

Index Terms— Myocardial mechanics, ventricular segmentation, myocardial stiffness, cardiac contractility, FE modelling

1. INTRODUCTION

The goal of this study was to develop methods for linking the finite element (FE) models of the heart (using the Auckland heart modelling approach) with population-based atlases of segmented 3D cardiac image data (from the UPF group in Barcelona) and spatial protein expression databases (from the MRC group in Edinburgh). This study forms part of the European FP-7 funded Ricordo project, which is being led by EBI in Cambridge who are also creating the annotation framework to be used by the FieldML and CellML models. Here, we provide proof of principle for enabling the anatomically and biophysically based FE models to be more specific to a particular patient. Such techniques can take advantage of population databases that characterise the shape of the heart for large numbers of patients. This paper describes the fully automated fitting of the Auckland 3D cardiac mechanics model to heart surface data extracted from the UPF population database, defined at the unloaded, end-diastolic (ED) and end-systolic (ES) states. Mechanical properties are fitted to the kinematic data to extract measures of the diastolic stiffness and systolic contractility of the heart by running mechanics solutions through the cardiac cycle. Ultimately, personalised estimates of the myocardial strain, stress and work distributions could be derived using this automated FE modelling framework.

2. METHODOLOGY

We used an unsupervised segmentation method to generate ventricular surface data for individual human hearts, to which we automatically fit a biomechanical FE model using nonlinear least squares and C^1 continuous shape functions. We demonstrate this approach using geometric data derived from multi-slice computed tomography (MSCT) images, but the data could alternatively be extracted from 3D statistical shape models [1] or 3D cardiac MRI [2]. We used the FE models to solve the governing equations for finite deformation continuum mechanics to simulate ventricular deformation throughout the cardiac cycle, and thus to extract global mechanical properties such as passive tissue stiffness and maximum myocardial contractility. The steps are summarised below.

2.1. Geometric Data

In this study, LV surfaces were extracted using non-rigid image registration of a manually segmented reference MSCT image with a patient's MSCT image. The deformation was modelled as a multi-scale set of B-splines, while the mutual information similarity measure was employed [3]. The reference segmentation, represented as a triangulated surface mesh, was subsequently warped according to this resulting deformation [4]. Like other anatomical imaging modalities, MSCT does not provide circumferential strain information.

In this study, the LV surfaces were extracted at three different stages of the cardiac cycle: diastasis, end-diastole, and end-systole.

2.2. Data and FE Model Alignment

The segmented surface data (Figure 1(a): green) described in section 2.1 underwent a rigid transformation in order to refer the data to a conventional cardiac coordinate system, in which the *x*-axis is aligned with the long-axis of the LV (passing from the centroid of the LV base through the LV apex); the *y*-axis is directed from the centroid of the LV to the centroid of the RV (near the mid-ventricle); and the *z*-axis is oriented in the anterior-to-posterior direction. Similar transformation procedures were applied to the ED and ES surface data.

In this study, we adapted an existing canine model with embedded myocardial fibre orientation fields [2] to fit to the human surface geometry data. The initial steps were to register and anisotropically scale the FE model to the human data as follows.

1) We generated a series of points spanning the epicardial and endocardial surfaces of the FE model (Figure 1(a) : gold), constructed a k-d tree [5] from these surface points, and used an iterative closest point method to determine the optimal transformation (translation, rotation, and anisotropic scaling) that best matched the model to human LV surface data.
2) The inverse rotation and translation was then applied to the scaled model and to the segmented surface data to transform them back the cardiac coordinate system of the initial FE model (Figure 1(b)).

The resulting scaled model provides a good initial model for a full nonlinear FE fitting procedure to construct a personalised LV model based on the segmentation data.

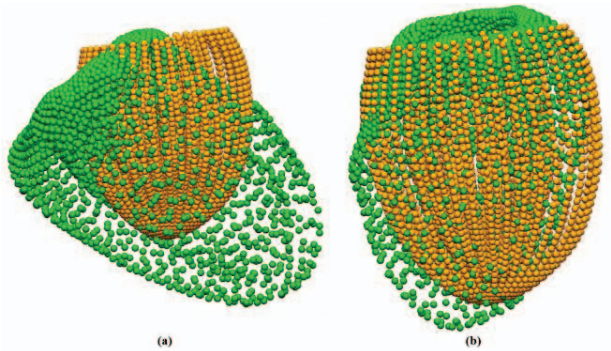


Figure 1: (a) Initial positions of segmented human LV surface data (green) and initial FE surface data (gold). (b) Alignment of human LV and model following rigid transformation of segmentation data, and anisotropic scaling of the FE model.

2.3. Model Fitting

We fitted the reference canine FE mechanics model to surface data segmented from the diastasis image using the methods detailed in [2]. The FE model consisted of 16 hexahedral finite elements (4 circumferential, 4 longitudinal and 1 radial element) interpolated using C^1 continuous basis functions. The human LV surface data were separately projected onto epicardial and endocardial surfaces of the scaled FE model. Nonlinear least-squares optimisation was used to adjust the geometric parameters of each FE model surface to best match the corresponding LV human data. Figure 2 shows the final fitted FE model superimposed with the segmented surface data.

Personalised measurements of myocardial fibre-sheet orientations were unavailable for this study. Therefore, in order to account for the LV myocardial architecture, we incorporated histologically derived fibre-sheet orientation data from the canine LV myocardium [2, 6].

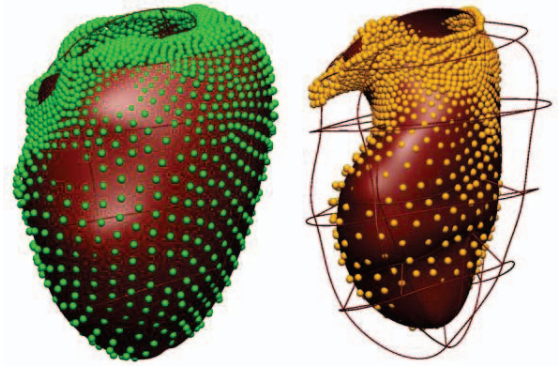


Figure 2: Personalised LV FE model (brown lines and surfaces) fitted to the human LV epicardial (left: green) and endocardial (right: gold) surface points.

2.4. LV Mechanics

LV mechanics was simulated in two phases: 1) passive diastolic filling; and 2) active systolic contraction, which included isovolumic contraction (IVC), ejection and isovolumic relaxation (IVR). The governing equations of finite deformation elasticity were solved using the finite element method (FEM). Myocardial mechanical properties were estimated on a patient-specific basis to provide estimates of the passive myocardial stiffness and active contractility.

2.4.1. Diastolic Mechanics and Passive Stiffness

Physiological boundary constraints (LV cavity pressure and displacement boundary conditions) were applied. The epicardial basal nodes of the model were constrained to match the motion of the segmented surface data. On the other hand, the apex was unconstrained. Due to the lack of *in vivo* pressure data in this study, pressure loading constraints were taken from other studies. To simulate

diastolic filling, 1 kPa [7] was applied to the LV endocardial surface of the reference FE model.

The passive mechanical behaviour was modelled using a transversely-isotropic exponential constitute equation [8]:

$$W = C_1 \exp(Q)$$

$$\text{where } Q = C_2 E_{ff}^2 + C_3(E_{cc}^2 + E_{rr}^2 + 2E_{cr}^2) + 2C_4(E_{fc}E_{cf} + E_{fr}E_{rf})$$

where $E_{\alpha\beta}$ are the components of Green's (Lagrange) strain tensor referred to fibre (f), cross-fibre (c) and radial (r) material coordinates, and C_1 - C_4 are the passive myocardial constitutive parameters. To tune the global stiffness (C_1), an optimisation was performed to best match the inflated FE mechanics model to the segmented ED surface data. After predicting the ED shape, the segmented data were projected onto their corresponding FE model surfaces, and the overall root-mean-squared error of the projections was then minimised by varying C_1. Other parameters describing the anisotropy (C_2 - C_4) were not included in the estimation due to the lack of regional strain information in the segmented data. Instead, their values were taken from our previous study based on MRI tagging in canine hearts [9].

2.4.2. Systolic Mechanics and Active Contractility

After tuning the passive properties, the simulation was continued through IVC, ejection, and to the end of IVR. Contraction of the LV model was driven by a calcium-dependent active tension transient (T_{Ca}) throughout systole. The contractile tension (T_a) was modelled using the following steady-state active tension model [10]:

$$T_a = T_{Ca}(1 + \beta(\lambda - 1))$$

where λ is the fibre extension ratio and β is a material parameter that describes the length-dependence of the contractile tension. Following the end of inflation, T_{Ca} was gradually increased to mimic the release of calcium from the sarcoplasmic reticulum (SR). During IVC, the cavity pressure was raised to counteract the contractile force in order to maintain the ED cavity volume. Simulations ran until the cavity pressure reached an afterload of 12 kPa [11]. The volume constraint was then relaxed so that the LV cavity could begin to eject. The ejection phase terminated when T_{Ca} reached its peak. T_{Ca} was then decreased to mimic the uptake of calcium back into the SR. The endocardial pressure was also lowered gradually during IVR to ensure that the cavity volume remained at the end-systolic volume.

One outcome of this study is an estimate of the maximum contractility (T_{Ca}) at ES. This was achieved by projecting the segmented ES surface data onto the simulated ES model, and varying T_{Ca} until the ES model best matched the human ES data.

3. RESULTS

For this case study example, the optimal value of C_1 was found to be 2.6 kPa and the maximum contractility (T_{Ca}) was estimated to be 110 kPa. The root-mean-squared errors (RMSE) for the estimation of these two parameters were 1.98 mm and 1.75 mm for the ED and ES states, respectively. Figure 3 illustrates the optimal ED (a) and ES (b) states with the epicardial (left) and endocardial (right) surface projections of the corresponding segmented surface data.

We also assessed the goodness-of-fit of the estimated mechanical properties by comparing the predicted ED and ES cavity volumes with those measured directly from the segmented data. The model predicted ED cavity volume was 114 ml compared to 111 ml calculated from the surface data. The model predicted ES cavity volume was 51 ml compared to 47 ml calculated from the ES surface data. Thus, the tuned model provided reasonably good estimates of the LV cavity volume measurements.

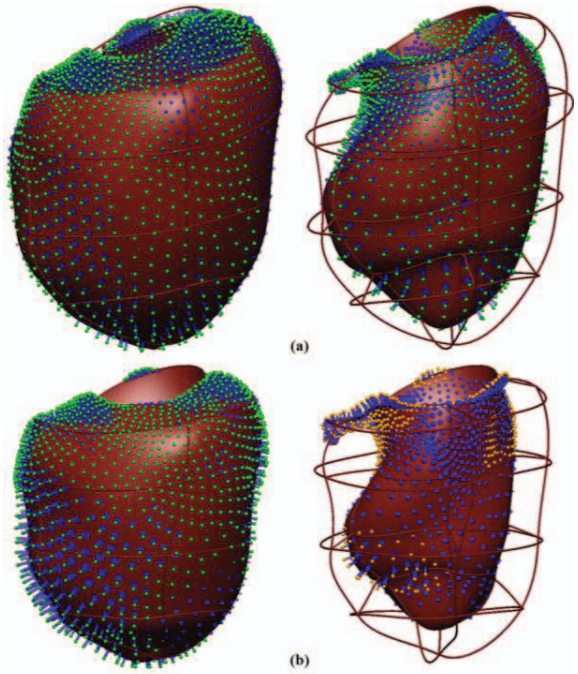


Figure 3: (a) Model predicted ED following passive parameter estimation with error projections (blue) of human ED surface data. (b) Model predicted ES following contractile parameter estimation with error projections of human ES surface data. (Left, epicard; Right, endocardium.)

To gain insight into regional ventricular function, we investigated the spatial variation of ES circumferential and radial strains (Figure 4), as well as the fibre strain and stress distributions (Figure 5). The ES circumferential strain (Figure 4(a)) was found to vary more heterogeneously across the LV wall compared to the fibre strain (Figure 5(a)). The radial strain (a measure of wall thickening) exhibited a significant transmural variation with greatest thickening in the sub-endocardial region. We also evaluated total fibre stress at ES (Figure 5(b)), which also exhibited a substantial transmural variation.

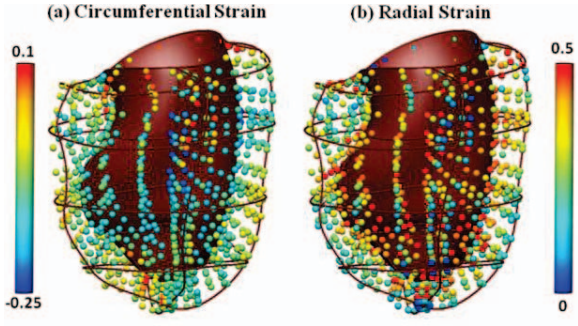


Figure 4: End-systolic circumferential (a) and radial strain distributions (b).

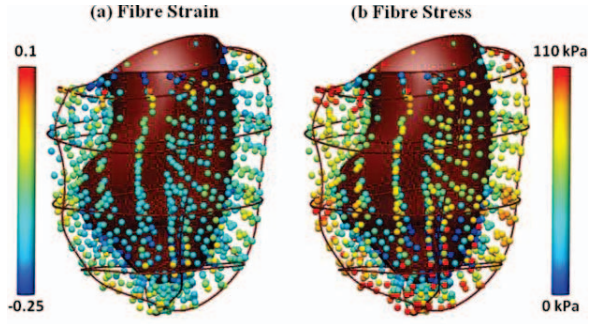


Figure 5: End-systolic fibre strain (a), and fibre stress distributions (b).

4. DISCUSSION AND CONCLUSIONS

We have developed methods to automatically segment cardiac surfaces from images of the human heart, and generate personalised FE biomechanics models of the LV in an unsupervised manner. Passive and active material parameters were tuned to best match the segmented ED and ES surface data, and the resulting myocardial strain and stress distributions were evaluated for the given individual.

Limitations of this study include a lack of endocardial pressure recordings, and lack of microstructural information for the human hearts studied. Pressure data were taken from the literature, and fibre-sheet orientation fields were adapted from an existing canine model.

This study forms part of the European FP7-funded Ricordo project, which is focused on the development of computational methods for linking biomechanical FE models, with atlas-based segmentation data, and protein expression data using novel ontological methods and CellML/FieldML model descriptions. The methods presented here form an important first step in this larger research collaboration by enabling the generation and simulation of personalised biomechanics, and extraction of individual-specific mechanical properties of human hearts. In particular, we are presently applying our methods to the Sunnybrook data (http://sourceforge.net/projects/cardiac-mr/files/) to determine the variations in mechanical properties between diseased and normal human hearts.

5. ACKNOWLEDGEMENTS

This work is funded by the European Commission's Ricordo project (FP7-ICT-248502), within the 7th Framework Programme. CH, GE and AFF have been partially funded by the Industrial and Technological Development Center (CDTI) CENIT-cvREMOD program, by the Spanish Ministry Science and Innovation under grant STIMATH (TIN2009-14536-C02-01), and by the European Commission's project euHeart (FP7-ICT-224495).

6. REFERENCES

[1] Tobon-Gomez C., Butakoff C., Aguade S., Sukno F., Moragas G., Frangi A.F. "Automatic construction of 3D-ASM intensity models by simulating image acquisition" *IEEE Trans on Medl Imag* 27(11):1655-1667, 2008.

[2] Wang, V., Lam, H., Ennis, D., Young, A., Nash, M.P. "Modelling passive diastolic mechanics with quantitative MRI of cardiac structure and function" *Med Imag Anal* 13(5):773-784, 2009.

[3] Rueckert, D., Sonoda, L.I., Hayes, C., Hill, D.L.G., Leach, M.O., Hawkes D.J. "Nonrigid registration using free-form deformations: Application to breast MR images" *IEEE Trans on Med Imag* 18(8):712-721, 1999.

[4] Ordas, S., Oubel, E., Leta, R., Carreras F., Frangi, A.F. "A statistical shape model of the heart and its application to model-based segmentation" *SPIE Med Imagg* 65111K, 2007.

[5] Greenspan, M., Yurick, M. "Approximate k-d tree search for efficient ICP" In *3-D Digital Imaging and Modeling Proceedings*, pp. 442-448, 2003.

[6] Nielsen P.M.F., Le Grice I.J., Smaill B.H., Hunter P.J. "Mathematical model of geometry and fibrous structure of the heart" *American J. Physiology* 260(4):H1365-H1378, 1991.

[7] Honda, H., Nakaya, S., Kamada, H., Hasegawa, H., Demachi, J., Chikama, H., Sugimura, K., Yamamoto, Y., Kumasaka, N., Takita, T., Ikeda, J., Kanai, H., Koiwa, Y., Shirato, K. "Non-invasive estimation of human left ventricular end-diastolic pressure" Medical Engineering and Physics 6:485-488, 1998.

[8] Guccione, J.M., McCulloch, A.D., Waldman, L.K. "Passive material properties of intact ventricular myocardium determined from a cylindrical model" Journal of Biomechanical Engineering 113:43-55, 1991.

[9] Wang, V.Y., Ennis, D.B., Young, A.A., Nash, M.P. "Modelling contractility and regional work throughout the cardiac cycle using FEM and MRI" *Lecture Notes in Computer Science* (in press), 2011.

[10] Hunter, P.J., McCulloch, A.D., ter Keurs, H.E.D.J. "Modelling the mechanical properties of cardiac muscle" *Prog in Biophysics and Mole Biol.* 69:289-331, 1998.

[11] McKay, R.G., Aroesty, J.M., Heller, G.V., Royal, H.D., Warren, S.E., Grossman, W., "Assessment of the end-systolic pressure-volume relationship in human beings with the use of a time-varying elastance model," *Circ,* 74:97-104, 1986.